On conformational analysis of chitosan

ARTICLE *in* CARBOHYDRATE POLYMERS · APRIL 2011

Impact Factor: 4.07 · DOI: 10.1016/j.carbpol.2011.01.011

2 AUTHORS:

Mirko X Weinhold
Universität Bremen
12 PUBLICATIONS **229** CITATIONS
SEE PROFILE

Jorg Thöming
Universität Bremen
97 PUBLICATIONS **1,337** CITATIONS
SEE PROFILE

Carbohydrate Polymers 84 (2011) 1237–1243

Contents lists available at ScienceDirect

Carbohydrate Polymers

journal homepage: www.elsevier.com/locate/carbpol

On conformational analysis of chitosan

Mirko X. Weinhold *, Jorg Thöming

UFT – Center for Environmental Research and Sustainable Technology, Leobener Strasse UFT, 28359 Bremen, Germany

ARTICLE INFO

Article history:
Received 20 October 2010
Received in revised form
16 December 2010
Accepted 10 January 2011
Available online 18 January 2011

Keywords:
Chitosan
Size-exclusion chromatography
Kuhn segment length
Persistence length
Conformational analysis

ABSTRACT

Chitosan, a natural polyelectrolyte with manyfold applications, is often described as a semi-flexible copolymer with linear chain behavior. Knowledge of the conformation of this polymer is relevant for viscosity-based molecular weight measurements as well as for gelation studies and use as thickener. However, conformational studies reveal a higher variety from compact to relatively stiff chain behavior than expected from the given structure. In this study, we found on the one hand semi-flexible chain behavior and on the other hand dextran-like compact behavior using a size-exclusion chromatography (SEC) system with online triple detection array (refractive index (RI), right and low angle light scattering (RALS, LALS) and viscometry detection). Using different theoretical models different Kuhn segment lengths l_K were found for the "semi-flexible" sample: 24 nm using the Benoit–Doty model and R_g-M data, 19 nm using the Odijk–Houwart model and R_g-M data as well as 17.5 nm using the Bohdanecký model and $[\eta]$–M data. Our results are in accordance with the expected behavior of semi-flexible linear chains from literature. However, the "compact" sample showed values of 9.8 nm in the high molecular weight part with similarity to reports on dextran.

1. Introduction

Conformation of polymers in solution influences strongly macroscopic polymer effects like viscosity. The elucidation of this dependence is important for understanding polymer functionalities and for designing semi-flexible and stiff polymers employed in the pharmaceutical, food, and chemical industries, as thickeners and for film forming.

The biopolymer chitosan, a cationic polyelectrolyte consisting of (1→4)-2-amino-2-deoxy-β-D-glucan (GlcN) and (1→4)-2-acetamido-2-deoxy-β-D-glucan (GlcNAc) units, is known as a relatively stiff polymer. It is usually produced by de-*N*-acetylation of chitin in hot alkali solutions. Depending on source of chitin and process parameters, different chitosan preparations are obtained with largely varying characteristics. Conformational aspects were studied by several groups; however, some specific chitosan dependant difficulties prevented a clear prediction which are in particular: a broad molecular weight distribution, missing standard samples, and solubility in a few solvents only. Up to now it is controversial whether the conformation of chitosan differs with the number of acetyl-groups (expressed as mole fraction of acetylation F_A) in respect to conformational parameters like persistence length L_p or Kuhn segment length l_K. Conformational analysis with different de-*N*-acetylated samples were carried out using the Mark–Houwink plot (M–H plot), where the molecular weight is plotted together against the intrinsic viscosity $[\eta]$ in a double logarithmic plot. The resulting Mark–Houwink (M–H) constants such as (a) and (K) indicate conformational changes of the analyzed polymer sample. In case of chitosan a literature survey reveals large differences in M–H constants and even contradictory results. Wang, Bo, Li, and Qin (1991) studied four samples with different F_A and observed linear M–H plots with the slope (a) between 0.81 and 1.12. In another study Anthonsen, Vårum, and Smidsrød (1993) found linear plots with (a) between 0.58 and 1.06 for three samples with different F_A. In both cases the decrease of F_A resulted in a decrease of the (a) value, which indicates an increasing stiffness for highly acetylated samples. On the contrary, Rinaudo, Milas, and Dung (1993) investigated three samples with different F_A but observed a linear plot with (a) of 0.93 and superimposition of all three samples. First indications for non-linear behaviors were observed by Chen and Tsaih (2000). They found breakpoints in the M–H plot in presence of different salts (urea). The (a) value changed here in one step from 0.68 to 1 at a specific molecular weight. Non-linear behavior but similar hydrodynamic behavior for samples with different F_A were also found by Berth, Dautzenberg, and Peter (1998). Within this report all samples showed a decrease of (a) with an increase of molecular weight. The slopes changed with no relation to the F_A from 0.5 to approx. 1 at the lowest molecular weight. Similar non-linear behavior was found by Weinhold et al. (Weinhold 2007, 2009) and Christensen, Vold, and Vårum (2008) with (a) values ranging from 0.5 to 1.2 and 0.8 to 1.15, respectively.

* Corresponding author. Tel.: +49 421 218 63389; fax: +49 421 218 8297.
E-mail address: mirkoweinhold@gmx.de (M.X. Weinhold).

0144-8617/$ – see front matter © 2011 Elsevier Ltd. All rights reserved.
doi:10.1016/j.carbpol.2011.01.011

Considering these strong deviations between reported literature values of M–H constants it is not surprising to find similar differences in reports about the Kuhn segment length l_K. Here values of 10 nm (Rinaudo et al., 1993), 12–25 nm (Berth et al., 1998), 22–30 nm (Brugnerotto, Desbrières, Heux, Mazeau, & Rinaudo, 2001) up to 60 nm (Rinaudo & Domard, 1989) and 30–80 nm (Terbojevich, Carraro, & Cosani, 1988) were reported, however, the rather high values could be ascribed to aggregated material later on. Previous reports found values between 8.6 and 11.6 nm (Schatz, Viton, Delair, Pichot, & Domard, 2003), 6 and 28.8 nm (Lamarque, Lucas, Viton, & Domard, 2005) and 8 and 16.4 nm (Christensen et al., 2008) if perturbed or unperturbed dimensions, different F_A and different degree of polymerizations DP were considered, respectively.

In this study we intend to elucidate polymer stiffness by a size exclusion chromatography (SEC) connected on-line with a triple detection array with right (90°) and low (7°) angle light scattering (RALS, LALS) and viscosimetry, in contrary to former investigations. The first part deals with the M–H behavior of unfractionated and fractionated commercial chitosan samples and its dependence on F_A. In the second part the experimentally obtained results on radius of gyration R_g and molecular weight M_W are compared to theoretical approaches in order to determine the stiffness parameter l_K for two samples.

2. Experimental

Material. Chitosan D [0.13] (the number in brackets denotes the F_A) were purchased from Chipro (Bremen, Germany), and Chi BU [0.19] was received from Heppe-Medical-Chitosan HMC (Halle, Germany). Sodium acetate, ethanol, acetic acid anhydride, ethylene glycol and acetic acid were obtained from Fluka (Germany). Ammonia (25%) was purchased from Merck KGaA (Germany). All reagents used were of analytical grade.

Preparations of re-N-acetylated samples. Initial chitosan was redissolved in 0.1 M acetic acid (200 mL) and diluted with methanol (250 mL). Then 50 mL methanol containing the amount of acetic anhydride required to give the target level of *N*-acetylation (calculated assuming a reaction efficiency of 100%). After stirring for 24 h at room temperature the product was precipitated by addition of diluted NH_3 solution and finally centrifuged. The samples were washed three times with water (pH = 10, NH_3 added) followed by freeze drying.

Purification of chitosan. Received chitosan preparations did sometimes contain a few percentage of insoluble matter. To get rid of this impurity insoluble matter was removed in the following way. Chitosan powder was dissolved in 0.5 M acetic acid (10 g/L) for 24 h. The clear solution was centrifuged 10 min (3577 × *g*) with an ultracentrifuge (Heraeus Instruments, Germany) and the supernatant was filtered through a 0.45 μm cellulose nitrate filter (Sartorius, Germany). The final products were then lyophilized.

Determination of the fraction of acetylation F_A . The F_A was determined by ^{1}H NMR spectroscopy according to the method of Hirai, Odani, and Nakajima (1991). Chitosan samples were dissolved in D_2O/DCl and NMR-spectra were recorded on a Bruker AVANCE WB-360 (8.4 T) spectrometer (360 MHz) and F_A values were obtained as described previously (Weinhold et al., 2009).

Molecular weight determination SEC[3] The biopolymer analysis was performed on a triple detection size-exclusion chromatography system (SEC[3], Viscotek, USA) consisting of an online two channel degasser, a high pressure pump, an autosampler (all parts integrated in the GPCmax, Viscotek, USA), a 0.5 μm stainless steel in-line filter with a nylon membrane, two serially connected ViscoGEL columns (PWXL mixed bed 6–13 μm methacrylate particles, 7.8 mm × 300 mm), a temperature controlled triple detector array (TDAmax 305, Viscotek, USA) with a differential refractometer at λ = 660 nm (RID 3580), a right angle (90°) light scattering detector (RALS) and a low angle (7°) light scattering detector (LALS 270-03) with a semiconductor laser diode at λ = 670 nm and a four capillary, differential Wheatstone bridge viscometer. The SEC conditions were as follows: a degassed 0.3 M CH_3COOH/0.3 M CH_3COONa buffer (pH = 4.5) with 1% ethylene glycol was used as eluent, the sample concentration was 0.3–1 mg/mL and samples were dissolved for 24 h under shaking, injection volumes varied from 10 to 100 μL, flow rate was maintained at 0.7 mL/min, and the column and detector temperature were kept at 30°C. Before injection, the sample solutions were filtered through a 0.45 μm cellulose nitrate disposable membrane (Sartorius, Germany). To ensure a low light scattering noise level the eluent was filtrated through a 16–40 μm glass filter. A polyethylene oxide standard (M_W = 22,411, [η] = 0.384 dL/g, M_W/M_N = 1.03) was used to normalize the viscometer and the light scattering detector. Data acquisition and processing were carried out by use of the OmniSEC 4.1 software (Viscotek Corporation). A dn/dc of 0.163 was used for the M_w calculation (Rinaudo et al., 1993). Within this study the laser was calibrated using R_θ of toluene (1.402×10^{-5} cm^{-1} obtained at 90° using 632.8 nm laser light (Kaye & McDaniel, 1974)).

At chitosan polymer radii higher than roughly 15 nm the intensity of the scattered light underlies an angular dependence. For this case the real molecular weight can only be obtained at 0° ($\sin^2(\theta/2) = 0$) of the backscattered light. However, this is technical impossible and the way to get the real molecular weight can be achieved with two strategies. First, the backscattered light is measured at more than three different angles (up to 18) and the molecular weight is obtained through different fitting methods and an extrapolation to ($\sin^2(\theta/2) = 0$). Second, the detector is orientated at a rather small angle (7°, ($\sin^2(\theta/2) = 0.0037$) and the measured light is treated as the 0° intensity without any curve fitting (the small error which applies here is ignored). In this study the molecular weight was determined according to the second strategy.

Fractionation of chitosan. The biopolymer fractions were made on a RI-SEC system (Knauer, Germany) with two serially connected columns (PSS Novema 3000 and 1000Å, 8 mm × 300 mm) or with one preparative column (PSS Novema 3000Å, 30 mm × 300 mm). The samples were detected by a differential refractometer (Knauer 2300, λ = 950 nm) and fractions were collected by a Retriever 500 fraction collector (Axel Semrau GmbH, Spockhövel, Germany). Received fractions were analyzed on the triple detection system afterwards.

1. Conformational analysis: Mark–Houwink plot. The intrinsic viscosity [η] measured in a specific solvent is related to the molecular weight *M* by the Mark–Houwink equation.

$$[\eta] = K \cdot M^a \quad (1)$$

The so-called Mark–Houwink constants (*K*) and (*a*) depend upon the type of polymer, solvent and the temperature used during the viscosity measurement. The plot of the log [η] vs. log *M* typically gives a straight line with slope (*a*) and intercept log (*K*). The slope (*a*) can vary from 0 (compact sphere) over 0.65–0.85 (random coil) to 1.8 (very stiff chain) revealing information about the polymer conformation in solution. Within the triple detection system values for molecular weight and intrinsic viscosities are determined constantly during a chromatographic run of one polydisperse sample. By use of separation columns molecules with different molecular weights are retained on the column depending on their hydrodynamic shape so that nearly monodisperse fractions enter the detector cell successively. The obtained data show a significant increase of data points in comparison to batch methods. It therefore allows an improved comparison with theoretical models and a more reliable conformational analysis than data obtained from polydisperse samples and batch methods.

2. Conformational analysis: Worm-like chain model. The conformation transition between random coils and rigid rods may be

explained by the Benoit–Doty (Benoit & Doty, 1953) theory for the Kratky–Porod (Kratky & Porod, 1949) chain or the wormlike polymer chains, which are the most typical models proposed for semiflexible polymers. According to the theory, R_g of unperturbed polymer chains is given by

$$R_g^2 = \frac{l_K L}{6} - \frac{l_K^2}{4} + \frac{l_K^3}{4L} \cdot \left[1 - \frac{l_K}{2L} \cdot (1 - e^{-2L/l_K})\right] \quad (2)$$

where l_K is the Kuhn segment length ($l_K = 2L_p$), which is used as a measure of chain stiffness of the polymer and L is the contour length defined as $L = M_W/M_L$ and $L = l_K N_K$ where N_K is the number of Kuhn segments. For a given l_K the L and R_g values can be calculated theoretically and are compared to a set of L and R_g data received from the experiment. When accordance between theory and experiment is found the l_K is obtained.

A convenient method to estimate L_p from the molar mass dependence of R_g is the Odijk–Houwart model Odijk & Houwart, 1978; Odijk, 1978. In the Odijk–Houwart model, the total persistence length $L_{p,T}$ of worm-like polyelectrolyte chains is the sum of two contributions:

$$L_{p,T} = L_{p,0} + L_{p,e} \quad (3)$$

$L_{p,0}$ is the intrinsic persistence length corresponding to an equivalent neutral chain in which all of the electrostatic interactions are screened out. The second one $L_{p,e}$ is the electrostatic contribution to the total persistence length due to the electrostatic short-range interactions, which depend on the ionic strength. The complete calculation to determine $L_{p,0}$ of a polyelectrolyte is reported by Fouissac, Milas, Rinaudo, and Borsali (1992), Mendichi, Šoltés, and Schieroni (2003) and Berth et al. (1998). We used the approximation of R_g^2 shown by Ghosh, Li, Reed, and Reed (1990) to calculate the contribution of the ionic strength and thus the intrinsic persistence length $L_{p,0}$:

$$R_g^2 = \frac{L}{3}\left(L_{p,0} + \frac{30.7}{C_s^{0.5}}\right) \quad (4)$$

where C_s is the salt concentration in mM and L the contour length. When accordance between theory and experiment is found the $L_{p,0}$ or $l_{K,0}$ is obtained.

3. Conformational analysis: Bohdanecký approach. To simplify the calculation procedures, we used the approximation of the wormlike chain model introduced by Bohdanecký (1983). According to the model, $(M^2/[\eta])^{1/3}$ is a linear function of $M^{1/2}$

$$\left(\frac{M^2}{[\eta]}\right)^{1/3} = A_\eta + B_\eta M^{1/2} \quad (5)$$

$$A_\eta = A_0 M_L \Phi_{0,\infty}^{-1/3} \quad (6)$$

$$B_\eta = B_0 \Phi_{0,\infty}^{-1/3}\left(\frac{2L_p}{M_L}\right)^{-1/2} \quad (7)$$

$\Phi_{0,\infty}$ is the limiting value of the Flory viscosity constant and equals 2.86×10^{23}. A_0 and B_0 are known functions of the reduced hydrodynamic diameter (d_r), and in practice B_0 can be replaced by a mean value (1.05). L_p (L_p = 0.5 l_K) is the persistence length, and M_L is the molar mass per unit of contour length which can be calculated as follows

$$M_L = \frac{F_A \cdot M_{GlcNAc} + (1 - F_A) \cdot M_{GlcN}}{b} \quad (8)$$

M_{GlcNAc} and M_{GlcN} are the monomer weights of intra-chain *N*-acetyl glucosamine (203 g/mol) and glucosamine (acetate salt, 221 g/mol) residues, respectively, and b is the average bond length (0.515 nm). Experimental data are plotted as described above and the obtained lines are fitted according to linear regression. From the resulting slope B_η the l_K can be calculated.

The hydrodynamic radius R_h was calculated through combination of online viscometer and the light scattering detector and resulted in R_h values for every elution slice:

$$R_h = \left[\frac{3}{4\pi}\left(\frac{[\eta]M}{0.025}\right)\right]^{1/3} \quad (9)$$

3. Results and discussion

3.1. Comparison of Mark–Houwink plots

Among six different chitosan preparations described elsewhere (Weinhold et al., 2009) we selected two samples for the conformational analysis including molecular weight and viscosity data in order to compare their Mark–Houwink plots (M–H) (Fig. 1b). As reported previously (Weinhold et al., 2009) every sample showed a non-linear M–H plot, however, with specific curvature for different samples. To highlight this effect we want to discuss the M–H plot of sample Chi D in detail, which showed the strongest curvature at decreasing slope for increasing molecular weight (Fig. 1b).

The rather strong decrease of the slope over the whole molecular weight range, found for sample Chi D, needs extra comment. Since chitosan shows a trend to aggregate in solution (Anthonsen, Vårum, Hermansson, Smidsrød, & Brant, 1994), an aggregation process would yield in a more compact material accompanied by a decrease of viscosity. Therefore, the expected effect would show similar effects on the M–H plot. However, strong pre-peaks in the detector responses (especially in the light scattering detector) and an increase or curvature of the log M distribution over the retention volume indicate the presence of aggregates. These effects were completely absent for the measured samples (see also electronic supplementary information). Yanagisawa, Kato, Yoshida, and Isogai (2006) showed that the absence of aggregates is an important prerequisite for a reliable conformational analysis. To avoid any accidentally occurrence of aggregated material we started to filter the sample solutions carefully. Although the sample solution was already filtered before analysis (0.45 μm) and the observed M–H plot was reproducible in several injections, we tried a further filtering to eliminate any uncertainty. The same sample solution was filtered (0.2 μm), injected in a semi-preparative chromatography system with two columns, fractions were collected and the eluted fraction was subsequently analyzed with the triple detector system described above. From the low polydispersity (1.1 up to 1.5) of the fractions we can exclude any possible entanglement between low and high molecular weight chains leading to an aggregation. Additionally, aggregates would collapse under such high shear stress (1.5 mL/min, three gel columns) or are not retained from the gel columns and filters, respectively. The fact that we received ideal Gaussian detector responses for the fractions (see electronic supplementary information) is in accordance to the identical overlay of the M–H segments in comparison to the initial sample (Fig. 1b). At no time we found an evidence that the observed curvature was caused by aggregated material.

Obtained plots showed nearly identical behavior for the initial sample as well as for the fractions with polydispersity indices between 1.15 and 1.41 (Fig. 1b and c). The highest fraction of 402 kg/mol had the lowest slope of 0.4 followed by 200 kg/mol with 0.57 and 126 kg/mol with 0.66. Fragments of the M–H plot showed a clear superimposition with data of the initial sample. Considering the Gaussian peak shapes without signs of bimodal distribution of the elution profiles as well as the linear behavior of log R_h and log M over the retention volume (Fig. 1a), we have no doubt that this behavior is no artefact and must be ascribed to some intrinsic property of the sample.

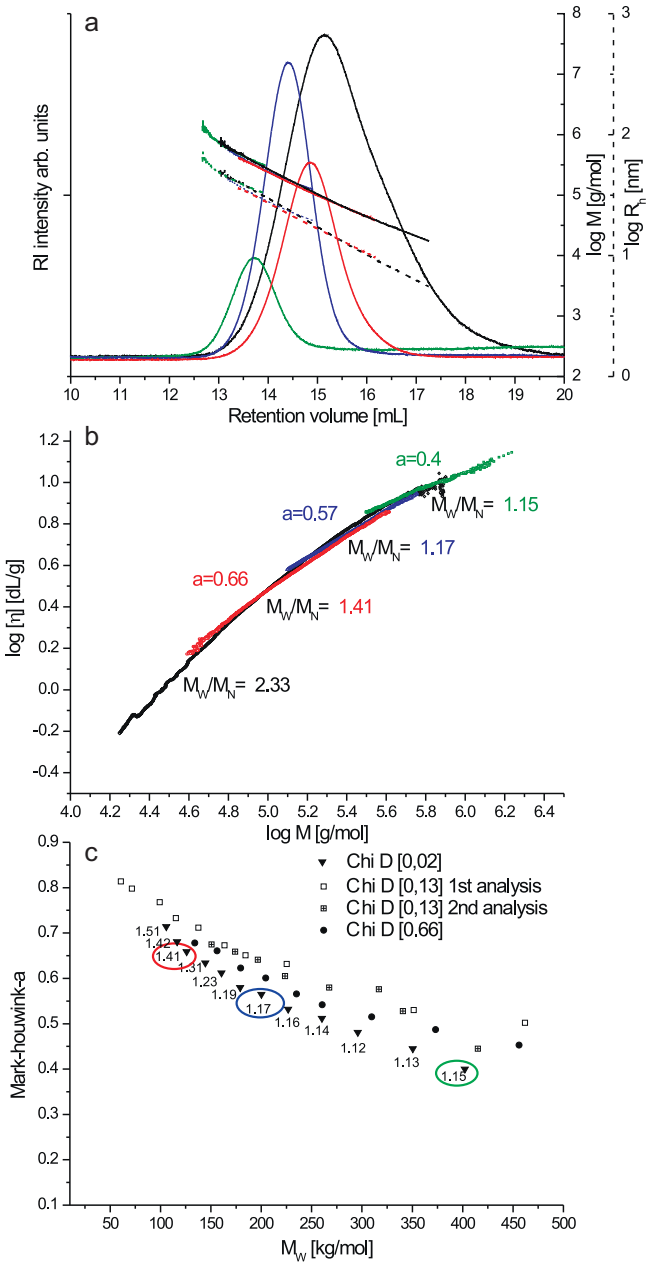

Fig. 1. Mark–Houwink plots. (a) Chromatogram of the initial sample Chi D (black) and three selected fractions (red, green blue) taken from this sample. (b) Mark–Houwink plots for every sample. The slope of every fraction as well as its polydispersity are shown. (c) Dependence of the M–H slope with the mean molecular weight of several fractions from Chi D with different F_A after re- or de-*N*-acetylation. The slope is decreasing with an increase of the molecular weight, however, comparison between different F_A with the same molecular weight show only slight dependency on F_A. Numbers in the plot refer to polydispersity indexes.

In order to investigate the dependence of the M–H slope on the F_A, Chi D was re- and de-*N*-acetylated and the obtained products were fractionated as described above. The slope of the fractions decreased with increasing molecular weight and only slight differences could be observed for different F_A indicating a small impact of F_A on conformation in a 0.3 M acetic acid buffer solution. This confirms results of previous studies (Berth et al., 1998; Yanagisawa et al., 2006; Christensen et al., 2008), which also observed little contribution to chain stiffness by a change of F_A.

More often the pattern of acetylation P_A is discussed to show some influence on conformation in solution. Block-wise distributed acetyl groups show a different charge distribution in comparison

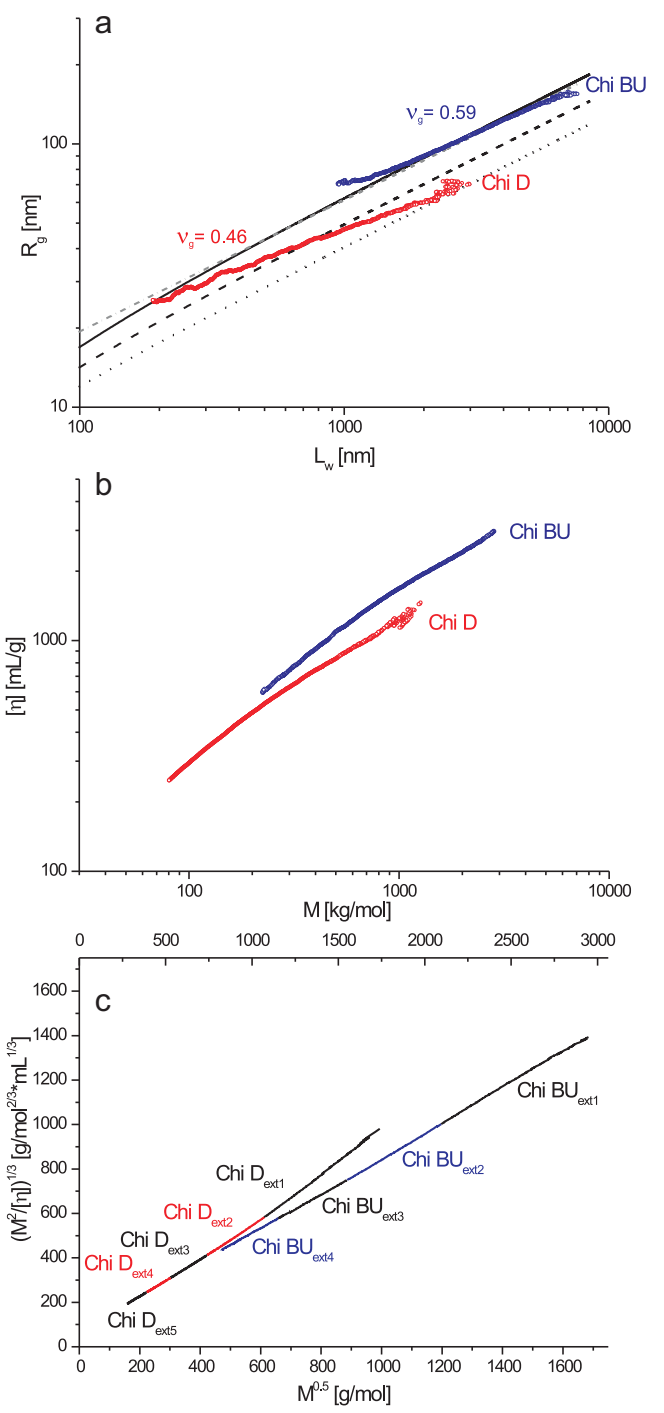

Fig. 2. Behavior of R_g in dependence of L_W. (a) Conformational plot using the worm-like chain model: radius of gyration (R_g) and contour lengths (L_w) are shown for three calculated curves with Kuhn segment lengths (l_K) of 24 nm (solid line), 15 nm (dashed line) and 10 nm (dotted line). The grey dash dotted line was obtained using Odijk's model with a l_K of 19 nm. Experimental values are shown for two different chitosan preparations Chi D (red open circles) and Chi BU (dark blue open circles). (b) Mark–Houwink plot for initial Chi BU as well as Chi D. (c) Bohdanecky plot for Chi BU and Chi D. Both lines were cut into four and five extracts, respectively, to improve the quality of the subsequential linear fit of the curved plot. Kuhn segment lengths (l_K) were determined for each extract separately (see Table 2). (For interpretation of the references to color in this figure legend, the reader is referred to the web version of the article.)

Table 1
Physicochemical parameters of the chitosan samples used for conformational analysis. M_W: weight averaged molecular weight, M_N:number averaged molecular weight, M_W/M_N: polydispersity, DP_W: degree of polymerization, F_A: fraction of acetylation, $[\eta]$: intrinsic viscosity, ν_g: slope of the R_g–M plot, M–H a: slope of the $[\eta]$–M plot, M_L: mass per unit of contour length, $R_{g,h}$: radius of gyration and hydrodynamic radius, respectively.

Sample	M_W [kg/mol]	M_N [kg/mol]	M_W/M_N	DP_W	F_A	$[\eta]$ [mL/g]	ν_g	M–H a	M_L [g/mol·nm]	R_g [nm	R_h [nm]
Chi BU	956	589	1.6	5262	0.19	1524	0.59	0.55–0.74	422	88	59
Chi D	112	48	2.4	641	0.13	282	0.46	0.47–1.0	424	27	16

to random copolymers. However, it could be shown that the used chitosan preparation showed completely random pattern characteristics (Weinhold, Sauvageau, Kumirska, & Thöming, 2009).

Thus, the observed curvature of the M–H plot could neither be correlated to a change of the F_A, a different pattern of acetylation P_A nor to an artefact of an aggregation process.

3.2. Comparison of experimental data with the worm-like chain model

In triple detection chromatography experiments the weight-averaged degree of polymerization DP_W (or L_W) of each elution slice can be measured simultaneously with the R_g (as well as R_h and $[\eta]$) of this specific slice. If ideal behavior during chromatography applies, molecules are separated linearly with their hydrodynamic shape and each elution slice can be considered as a nearly monodisperse fraction. This yields into a set of numerous data with given parameters (L_W, R_g) for almost monodisperse fractions which cover a broad molecular weight range (depending on the overall M_W/M_N of the sample). These data can be easily compared to theoretical approaches like the worm-like chain model where R_g can be calculated for semi-flexible polymer chains. The advantage of this comparison is that stiffness parameters like the persistence length L_p or the Kuhn segment length l_K can be deduced from the theoretical curve if superimposition with experimental data is found.

Fig. 2a shows the comparison of two different chitosan preparations Chi BU and Chi D. Conformation plots (R_g vs. L_W) were shown for each sample together with three calculated curves according to the Benoit–Doty model with Kuhn segment lengths (l_K) of 24 nm (solid line), 15 nm (dashed line) and 10 nm (dotted line) according to Eq. (2). The experimental curve of Chi BU and the theoretical curve for l_K of 24 nm showed almost identical behavior. Some deviations can be seen at the highest and lowest branch of the line, which can be attributed to low polymer concentration at the edges of the chromatographic peak. Using Eq. (4) for the calculation of the intrinsic Kuhn segment lengths ($l_{K,0}$) (grey dashed-dotted line in Fig. 2a) a perfect overlay with experimental data of Chi BU is obtained for a value of 19 nm. More interesting, the experimental curve of Chi D shows a complete different behavior. The slope of this curve is too low to fit to one of the theoretical curves and crosses all three curves instead. According to the Benoit–Doty model the l_K for Chi BU is 24 nm and $l_{K,0}$ is 19 nm using the Odijk–Houwart model, respectively. However, it was not possible to predict a constant l_K for Chi D, since there is no accordance to a single theoretical curve. Moreover this problem illustrates how difficult it is to obtain precise stiffness parameters from this method, especially for non-standard polymer behavior, so that we decided to apply a variant or simplification of the worm-like chain model introduced by Bohdanecký.

3.3. Comparison of stiffness parameters using Bohdanecký's simplification

The main advantage of the Bohdanecký approach is to get l_K values in a more convenient and more accurate way by fitting experimental curves and calculation of l_K from the slope of these curves. However, this requires not only molecular weight data but also viscosity data for the same slice fractions. Thanks to the application of a triple detector chromatography system this is no serious problem. Due to this we could use exactly the same set of data we used for the comparison of the Benoit–Doty model (Table 1).

The curve of Chi D exhibited a strong curvature in the Bohdanecký plot similar to the curvature in the M–H plot shown before (Fig. 2c). To be able to fit this curved plot more accurate, we cut the set of data in four and five extracts for both samples, respectively. For these extracts linear curve fitting was used and received results are summarized in Table 2. The "low" molecular weight regime of Chi BU (226–430 kg/mol) showed the highest l_K value of 18.8 nm and decreased only slightly in the rather high molecular weight regime (1433–2837 kg/mol) to 16.4 nm. Similar values of 17.2 nm were found for the low molecular weight regime (25–49 kg/mol) of Chi D. However, at increasing molecular weight the l_K drops quite strongly to the lowest value of 9.8 nm (370–980 kg/mol).

Comparing the average value of Chi BU 17.5 nm with the values obtained from Benoit–Doty (24 nm) and Odijk–Houwart model (19 nm) reveals a tendency to a lower segment length after use of $[\eta]$–M data than for R_g–M data. A similar effect was also observed by Mendichi et al. (2003). However, the values of Chi D differ again especially in the high molecular weight regime where the segment length is just the half of the length of Chi BU for comparable molecular weights (9.8 nm vs. 18.2 nm). For low molecular weights the segment length (17.3 nm) seems to adopt the Chi BU average value of 17.5 nm. This finding is similar to data of dextran (Ioan, Aberle, & Burchard, 2000). Power law behavior seems to be approached only in the small molar mass region. The effect of branching in dextran becomes noticeable at molar masses roughly between 10^4 and

Table 2
Parameters of chitosan extracts of two different chitosan preparations (Chi D and Chi BU). B_η: slope of the Bohdanecký plot (see Fig. 2c), F_A: fraction of acetylation, M_L: molar mass per contour length, l_K: Kuhn segment length, L_p: persistence length, highest/lowest M: upper and lowest molecular weight of the selected extracts, R^2: correlation coefficient from the linear fit in Fig. 2c.

Chitosan extracts	B_η [$g^{1/2}/mol^{1/6}\,mL^{1/3}$]	F_A	M_L [g/mol nm]	l_K [nm]	L_p [nm]	Highest M [kg/mol]	Lowest M	R^2
Chi BU_{ext1}	0.808	0.19	422	16.4	8.2	2837	1433	0.9995
Chi BU_{ext2}	0.810	0.19	422	16.4	8.2	1433	780	0.9999
Chi BU_{ext3}	0.768	0.19	422	18.2	9.1	780	432	0.9995
Chi BU_{ext4}	0.755	0.19	422	18.8	9.4	430	226	0.9996
Chi D_{ext1}	1.048	0.13	424	9.8	4.9	980	370	0.9995
Chi D_{ext2}	0.900	0.13	424	13.4	6.7	370	170	0.9998
Chi D_{ext3}	0.845	0.13	424	15.2	7.6	170	90	1
Chi D_{ext4}	0.821	0.13	424	16.0	8.0	90	49	0.9999
Chi D_{ext5}	0.790	0.13	424	17.2	8.6	49	25	0.9986

Table 3
Comparison of stiffness parameters of cellulose type (β-1→4) polymers obtained from literature using R_g–M as well as [η]–M data.

Type of polymer	Solvent	l_K [nm] from (R_g-M data)	l_K [nm] from ([η]–M data)	Source
Chitosan	0.3 M HAc/NaAc	19–24	9.8–18.8	this work
Chitosan	0.2 M HAc/NH_4Ac	8–16.4	10.2–16.2	Christensen et al., 2008
Chitosan	0.2 M HAc/ 0.15 M NH_4Ac	6–28.8		Lamarque et al., 2005
Chitosan	0.2 M HAc/NaAc		32	Morris, Castile, Smith, Adams, & Harding, 2009
Chitin	2.77 M NaOH	23.3–26.2		Einbu, 2004
Cellulose	LiOH/urea		12.2	Cai, Liu & Zhang, 2006
Cellulose	1% LiCl/DMI	18		Yanagisawa & Isogai, 2005
Hyaluronan	0.1 M NH_4NO_3	16	9	Fouissac et al., 1992
Hyaluronan	0.15 M NaCl +0 to 1 M NaOH	17.4		Ghosh, Kobal, Zanette, & Reed, 1993
Hyaluronan	0.15 M NaCl	15	13.6	Mendichi, Šoltés, & Schieroni, 2003
Galactomannans	0.1 M $NaNO_3$		11	Pollard, Eder, Fischer, & Windhab, 2010
Galactomannans	0.1 M $NaNO_3$		16–20	Morris et al., 2008

10^5 g/mol while at lower molecular weights the chain shows its linear power law behavior. The second similarity was found in the exponent ν from R_g–M dependence (Fig. 2a). Values for dextran (0.40–0.44; Ioan et al., 2000) are comparable to the found value of Chi D (0.46), in contrast, the exponent of Chi BU (0.59) is identical to the value typical found for linear chains (0.588; Burchard, 2001). Apart from this, similar effects could be seen for the typical linear polymer cellulose (Yanagisawa, Shibata & Isogai, 2005). While several cellulose pulp samples had exponents between 0.57 and 0.59 in this publication, the softwood bleached kraft pulp (SBKP) showed also a quite low slope in the high molecular weight region (0.41). The authors concluded that some compact structures like branches or cross-linkages are present in the high molecular weight region of this sample.

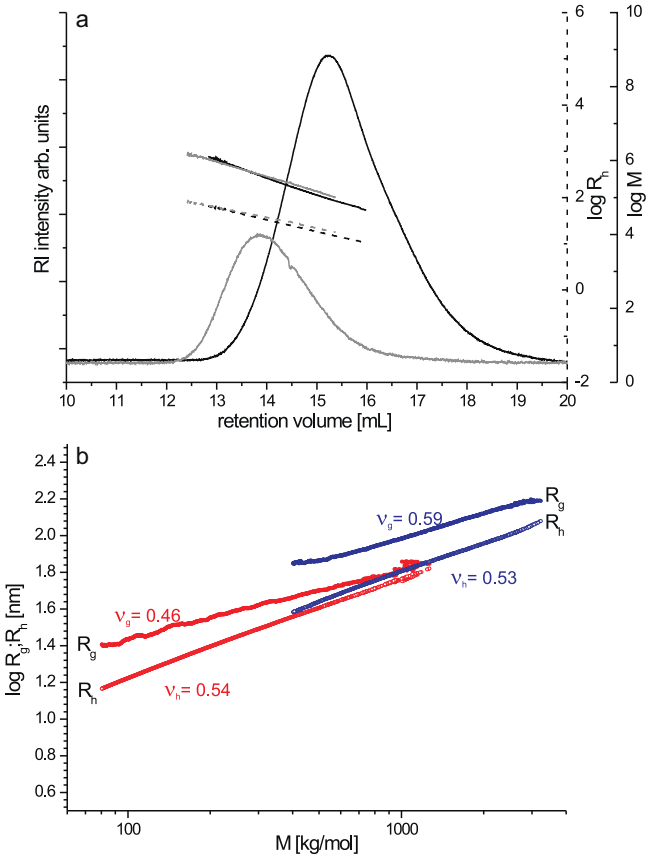

Fig. 3. Elution behavior. (a) RI-chromatograms of Chi BU (grey) and Chi D (black). (b) Behavior of the hydrodynamic radius R_h and radius of gyration R_g for sample D and BU.

The radii of gyration R_g and the hydrodynamic radius R_h are plotted against the molar mass M in Fig. 3b. Chi BU shows parallel lines for both radii which are generally found for linear chains (Schmidt & Burchard, 1981) (Fig. 3b). Strikingly, the curves for Chi D have not the same slopes (ν_g = 0.46, ν_h = 0.54) and convergent behavior of the lines is typically found in branched molecules (Galinsky & Burchard, 1995; Ioan et al., 2000). At low molecular weights no difference between both samples are visible likewise for l_K obtained from the Bohdanecký plot.

According to the conformational analysis, which incorporates R_g, R_h, [η] and M data, we found a significant deviation from linear chain behavior for Chi D in contrast to Chi BU. Additionally, in Fig. 3a the different hydrodynamic-mass relation of both samples eluted by chromatography can be recognized. Both lines intersect so that at low retention times Chi D shows slightly higher molar mass than Chi BU for the same elution slice at similar hydrodynamic shape.

Recent studies (Einbu, 2004) of chitin showed linear power law behavior and l_K values (R_g–M data) comparable to findings of Chi BU (Table 3). The conformational deviation from linear chain behavior of the high molecular weight part of Chi D may be explained by appearance of some branches or cross-linkages in the molecule so that they behave different than molecular-dispersed states. On the one hand, it needs to be clarified whether occurrence of slightly branched chains may vary with the source of chitin in different organisms and can be considered as a natural but rare property of chitin. On the other hand, it may appear during reaction in concentrated NaOH solutions used for de-*N*-acetylation and the branching or cross-linking is a process-induced effect.

4. Conclusion

Within this study a complete conformational analysis using R_g, R_h, [η] and M data was shown on two samples. For Chi BU Kuhn segment lengths l_K of 24 nm, 19 nm and 17.5 nm using the Benoit–Doty model and R_g–M data, the Odijk–Houwart model and R_g–M data and the Bohdanecký model and [η]–M data were found, respectively. Obtained results are comparable to literature values for chitosan as well as for cellulose type polymers (Table 3). Power law behavior was found to be in accordance with the expected behavior of semi-flexible linear chains. Deviations from this behavior were observed for the second sample Chi D with comparable characteristics to branched macromolecules like dextran. At low molecular weights similar power law behavior to the first sample were found with a l_K of 17.3 nm (Bohdanecký model and [η]–M data). However, at high molecular weights the l_K decreased to 9.8 nm. Although chitin and chitosan are typically described as linear copolymers, we

could show for the first time that not all chitosan preparations show a linear chitin structure. Thus, this effect could be a reason for the high variety of stiffness parameters and Mark–Houwink constants found for this class of polymer in literature.

Acknowledgements

We would like to acknowledge Raphael Böhm, Alexander Mauer, Jan Tell, Thomas Veltzke, Andrea Kück and Daniel Waterkamp for assistance in chitosan preparation. Financial support provided by the Deutsche Bundesstiftung Umwelt (DBU) under grant AZ 25832 is also gratefully acknowledged.

Appendix A. Supplementary Data

Supplementary data associated with this article can be found, in the online version, at doi:10.1016/j.carbpol.2011.01.011.

References

Anthonsen, M., Vårum, K., & Smidsrød, O. (1993). *Carbohydrate Polymers*, *22*, 193–201.
Anthonsen, M., Vårum, K., Hermansson, A., Smidsrød, O., & Brant, D. (1994). *Carbohydrate Polymers*, *25*, 13–23.
Benoit, H., & Doty, P. (1953). *The Journal of Physical Chemistry*, *57*, 958–963.
Berth, G., Dautzenberg, H., & Peter, M. (1998). *Carbohydrate Polymers*, *36*, 205–216.
Bohdanecký, M. (1983). *Macromolecules*, *16*, 1483.
Brugnerotto, J., Desbrières, J., Heux, L., Mazeau, K., & Rinaudo, M. (2001). *Macromolecular Symposia*, *168*, 1–20.
Burchard, W. (2001). *Biomacromolecules*, *2*, 342–353.
Cai, J., Liu, Y., & Zhang, L. (2006). *Journal of Polymer Science B: Polymer Physics*, *44*, 3093–3101.
Chen, R., & Tsaih, M. (2000). *Journal of Applied Polymer Science*, *75*, 452–457.
Christensen, B., Vold, I., & Vårum, K. (2008). *Carbohydrate Polymers*, *74*, 559–565.
Einbu. (2004). *Biomacromolecules*, *5*, 2048–2054.
Fouissac, E., Milas, M., Rinaudo, M., & Borsali, R. (1992). *Macromolecules*, *25*, 5613–5617.
Galinsky, G., & Burchard, W. (1995). *Macromolecules*, *28*, 2363–2370.
Ghosh, S., Li, X., Reed, C., & Reed, W. (1990). *Biopolymers*, *30*, 1101.
Ghosh, S., Kobal, I., Zanette, D., & Reed, W. (1993). *Macromolecules*, *26*, 4685.
Hirai, A., Odani, H., & Nakajima, A. (1991). *Polymer Bulletin*, *26*, 87.
Ioan, C., Aberle, T., & Burchard, W. (2000). *Macromolecules*, *33*, 5730–5739.
Kaye, W., & McDaniel, J. (1934–1937). *Applied Optics*, *13*
Kratky, O., & Porod, G. (1949). *Rev. Trav. Chim. Pays-Bas.*, *68*, 1106–1123.
Lamarque, G., Lucas, J.-M., Viton, C., & Domard, A. (2005). *Biomacromolecules*, *6*, 131–142.
Mendichi, R., Šoltés, L., & Schieroni, A. (2003). *Biomacromolecules*, *4*, 1805–1810.
Morris, G. A., Patel, T. R., Picout, D. R., Ross-Murphy, S. B., Ortega, A., & Garcia de la Torre. (2008). *Carbohydrate Polymers*, *72*, 356–360.
Morris, G. A., Castile, J., Smith, A., Adams, G. G., & Harding, S. E. (2009). *Carbohydrate Polymers*, *76*, 616–621.
Odijk, T., & Houwart, A. (1978). *Journal of Polymer Science: Polymer Physics Edition*, *16*, 627–639.
Odijk, T. (1978). *Polymer*, *19*, 989.
Pollard, M. A., Eder, B., Fischer, P., & Windhab, E. J. (2010). *Carbohydrate Polymers*, *79*, 70–84.
Rinaudo, M., Milas, M., & Dung, P. (1993). *International Journal of Biological Macromolecules*, *15*, 281–285.
Rinaudo, M., & Domard, A. (1989). *Chitin and Chitosan*. Amsterdam: Elsevier., p.71.
Schatz, C., Viton, C., Delair, T., Pichot, C., & Domard, A. (2003). *Biomacromolecules*, *4*, 641–648.
Schmidt, M., & Burchard, W. (1981). *Macromolecules*, *14*, 210.
Terbojevich, M., Carraro, C., & Cosani, A. (1988). *Carbohydrate Research*, *180*, 73.
Wang, W., Bo, S., Li, S., & Qin, W. (1991). *International Journal of Biological Macromolecules*, *13*, 281–285.
Weinhold, M., Sauvageau, J., Tartsch, B., Clarke, P., Jastorff, B., & Thöming, J. (2007). *Advances in Chitin Science*, *10*, 66–71.
Weinhold, M., Sauvageau, J., Keddig, N., Matzke, M., Tartsch, B., Grunwald, I., Kübel, C., Jastorff, B., & Thöming, J. (2009). *Green Chemistry*, *11*, 498–509.
Weinhold, M., Sauvageau, J., Kumirska, J., & Thöming, J. (2009). *Carbohydrate Polymers*, *78*, 678–684.
Yanagisawa, M., Kato, Y., Yoshida, Y., & Isogai, A. (2006). *Carbohydrate Polymers*, *66*, 192–198.
Yanagisawa, M., & Isogai, A. (2005). *Biomacromolecules*, *6*, 1258–1265.
Yanagisawa, M., Shibata, I., & Isogai, A. (2005). *Cellulose*, *12*, 151–158.